NASA TECHNICAL MEMORANDUM

NASA TM X-71658

NASA TM X-71658

STATUS OF THE NASA-LEWIS FLAT-PLATE COLLECTOR TESTS WITH A SOLAR SIMULATOR

by F. F. Simon
Lewis Research Center
Cleveland, Ohio 44135

TECHNICAL PAPER presented at
NSF/RANN Workshop on Solar Collectors for
Heating and Cooling of Buildings
New York, New York, November 21-23, 1974

STATUS OF THE NASA-LEWIS FLAT-PLATE COLLECTOR TESTS WITH A SOLAR SIMULATOR

by F. F. Simon

National Aeronautics and Space Administration
Lewis Research Center
Cleveland, Ohio

E-8205

ABSTRACT

Simulator test results of 15 collector types are reported. Collectors are given performance ratings according to their use for pool heating, hot water, absorption A/C or heating and solar Rankine machines. Collectors found to be good performers in the above categories, except for pool heating, were a black nickel coated, 2 glass collector, and a black paint 2 glass collector containing a mylar honeycomb. For pool heating, a black paint, one glass collector was found to be the best performer.

Collector performance parameters of 5 collector types were determined to aid in explaining the factors that govern performance. The two factors that had the greatest effect on collector performance were the collector heat loss and the coating absorptivity.

INTRODUCTION

An area presently being investigated by the NASA-LeRC in its efforts to aid in the utilization of alternate energy sources, is the use of solar energy for the heating and cooling of buildings. An important part of the solar heating and cooling effort at the Lewis Research Center is the investigation of flat-plate collectors which have the potential to be efficient, economical, and reliable. Efficient collectors will be an important consideration in the realization of effective solar cooling systems.

The approach being taken at the Lewis Research Center for determining collector performance is to test collectors under simulated (indoor) and actual (outdoor) conditions. This paper reports the results to date of the collectors tested at Lewis under simulated sun conditions. The initial results reported in reference 1 are included herein as part of this status report.

COLLECTORS TESTED

A list of collectors tested to date is given in table I. The fifteen collector types listed in table I differ according to coating (non-selective or flat black paint, CuO coating, black nickel selective coating), type of glazing material (glass or Tedlar), number of cover sheets (1 or 2), type of absorber plate material (aluminum, steel or copper), and the use of mylar honeycomb material. The performance results for collectors 1 to 4 were previously reported (ref. 1).

EXPERIMENTAL METHOD

Experimental Facility

A drawing and a photograph of the facility are presented in figures 1 and 2. The primary components of the facility are the energy source (solar simulator), the liquid flow loop, and the instrumentation and data acquisition equipment. A summary of information describing the facility is presented in table II.

Solar Simulator

The basic rationale for the use of a solar simulator for the testing of solar collectors was given in reference 2. This approach allows for controlled conditions that makes it possible to properly compare the performance of different collector types. The simulator shown in figure 2 consists of 143 tungsten halogen 300 watt lamps placed in a modular array with Fresnel lenses placed at the focal distance so as to collimate the radiation.

A comparison of spectral characteristics of the simulator output with air mass-2 sunlight is given in table III. Table III demonstrates that the solar simulator does an excellent job of simulating the sun's radiation. More detailed information is given in reference 3.

Coolant Flow Loop

The flow loop consists of storage and expansion tanks, pump, heater, test collector, and the required piping shown schematically in figure 3. The hot fluid storage tank is a commercially available water heater for home use. The tank has two electrical immersion heaters, 5 kilowatts each, and has a capacity of 80 gallons. The pump is a gear type unit driven by a 1/4 horsepower electric motor through a variable speed drive.

A heat exchanger using city water as a coolant is used to control the temperature of the collector coolant fluid at the collector inlet.

A 50/50 by weight mixture of ethylene-glycol and water is used in the liquid loop. The specific gravity of the mixture is checked with a precision grade hydrometer. To suppress vapor formation the entire flow loop is pressurized to approximately 15 psig by applying a regulated inert gas pressure to the top of the expansion tank.

The collector to be tested is mounted on a support stand that allows rotation about either the horizontal axis or the vertical axis. This permits variation of the incident angle of the radiant energy to simulate both seasonal and daily variations, if desired.

Instrumentation and Data Acquisition

The parameters needed to evaluate collector performance are: liquid flow rate, liquid inlet and outlet temperatures, the simulated solar flux, wind speed, and the ambient temperature. The flow rate is determined with a calibrated turbine-type flow meter that has an accuracy better than one percent of the indicated flow. The collector inlet and outlet temperatures are measured with ISA type E thermocouples (chromel-constantan). The thermocouples were calibrated at 32° and 212° F. The

error in absolute temperature measurement is less than 1^{o} F and the differential temperature error between the inlet and outlet thermocouples was less than 0.2^{o} F.

The ambient temperature is measured with an ISA type E thermocouple mounted in a radiation shield. The simulated solar flux is measured with a water-cooled Gardon type radiometer having a sapphire window. The radiometer was calibrated with a National Bureau of Standards irradiance standard.

In addition to the measurements of the basic parameters mentioned above, the following parameters are also measured for the purpose of obtaining detail information.

1. Collector absorber plate temperatures
2. Collector glass temperatures
3. Collector coolant pressure and pressure drop
4. Temperature of surroundings

The millivolt-level electrical outputs of the measuring instruments are recorded on magnetic tape by the use of a high speed data acquisition system. The information from the tape is sent to a digital computer for data reduction and computation. The computer results are printed out in the test facility within minutes after the data is initially recorded.

Test Procedure

The collectors are mounted on the test stand and positioned so that the radiant flux is either normal to or at different angles to the collector. Variation of the incident angle is accomplished by rotating the test stand about the vertical axis. The present tests were run at an incident angle of zero degrees and a tilt angle of 57 degrees. The flow rate is adjusted to a value corresponding to 10 pounds per hour per square foot of collector absorber area. Before the simulator is turned on, the collector is given time to achieve thermal equilibrium at the inlet temperature chosen (1 hr or more). After thermal equilibrium is established for a given inlet temperature, the simulator is turned on and the desired radiant flux is obtained

by adjusting the lamp voltage. After steady-state conditions occur, usually in 10 to 15 minutes, data are recorded. The radiant flux is then readjusted to a second value at the same collector inlet temperature, steady-state conditions obtained, and data again recorded. The collector inlet temperature is then set to another value, and the procedure repeated.

COLLECTOR TEST RESULTS AND DISCUSSION

The experimental efficiency of each collector was calculated using the following equation:

$$\eta = GC_p(T_0 - T_1)/q_i \tag{1}$$

The efficiency determined for a constant flow rate of 10 lb/hr ft^2 was plotted against the temperature difference to heat flux ratio for an inlet temperature ranging between 75^o to 210^o F, a simulated heat flux ranging between 150 to 340 Btu/hr ft^2, wind speed of 7 mph and an ambient temperature ranging between 75^o F in winter to 85^o F in summer.

Correlative method. - Justification for the method of correlating collector test data was presented in reference 2. Basically the method involves the utilization of the analytical equations that describe collector performance. The three equations useful for obtaining key collector parameters are as follows:

$$\eta = \alpha\tau - U_L(\bar{T}_p - T_a)/q_i \tag{2}$$

$$\eta = F'\left[\alpha\tau - U_L(\bar{T}_f - T_a)/q_i\right] \tag{3}$$

$$\eta = F_R\left[\alpha\tau - U_L(T_1 - T_a)/q_i\right] \tag{4}$$

Examples of how these equations can be used in conjunction with the experimental data were given in references 2 and 4. Performance curves

of a black nickel two-glass collector (No. 7, table IV) from reference 4 are shown in figures 4(a) to (c). From an inspection of equations (2) to (4) it can be seen that by plotting efficiency against temperature difference divided by radiant flux (η against $(T - T_a)/q$) as indicated in figure 4, it is possible to obtain key collector parameters from the slope and intercept of the correlating lines. As explained in reference 2, the values of $\alpha\tau$, U_L, F', and F_R obtained in the above manner will give specific information on why a collector excelled or why it performed poorly.

Collector efficiency curves. - The efficiency in terms of the inlet temperature and radiant flux level for the fifteen collectors tested is shown in figure 5. The appearance of the curves of figure 5 points out the large differences that exist among the collectors tested. It is apparent that no one collector design has the highest efficiency throughout the entire range of the abscissa.

This is due to two considerations in evaluating performance; considerations that are not always compatible. One consideration is the slope of the curves which is a measure of the heat loss. It is seen from figure 5 that those collectors with a single cover have a larger slope and therefore a larger heat loss than those with two covers (e.g., No. 8 against No. 9). Larger heat losses are found for coatings having higher emissivity values (flat black coatings as contrasted to selective surface coatings, No. 10 against No. 5). The second consideration is coating absorptivity (α) and cover transmittance (τ). Collectors with two covers while decreasing heat loss also lower the cover transmittance as compared to single cover collectors. For comparable absorptivity values, the product of $\alpha\tau$ is lower for the two-cover collector compared to the single covered ones. This results in the two-cover collector having lower values of the performance curve intercept and higher efficiencies at higher values of the abscissa due to lower heat losses. The single covered collectors are higher performers at lower inlet temperatures, but a crossover point is reached whereby at higher abscissa values the double-covered collectors become better

performers. This effect is seen in comparing No. 11 with No. 12, No. 2 with No. 4, and No. 10 with No. 13. If transmittance is comparable the efficiency values at the intercept of figure 5 is directly related to the absorptivity of the surface. There will be further discussion on this point later in this report.

Collector performance ranking. - From the performance curves of figure 5, collector efficiency may be determined for the different functions a collector might be required to perform. The different functions considered for the purpose of performance ranking are heating of swimming pools ($T_i = T_a = 80^o$ F), generation of hot water ($T_i = 140^o$ F, $T_a = 80^o$ F), heating ($T_i = 120^o$ F, $T_a = 0^o$ F), absorption A/C ($T_i = 200^o$ F, $T_a = 80^o$ F), and using the collector thermal output for running a solar Rankine machine ($T_i = 240^o$ F, $T_a = 80^o$ F). The resulting calculations using figure 5 are shown in tables IV(a) to (d). All ambients are 80^o F except for the heating case which is 0^o F. This lower value of the ambient temperature introduces an error of approximately eight percent in the calculation of performance because the performance curves of figure 5 were obtained at a higher ambient temperature. This error does not change the order of performance ranking for heating and is therefore not important in the present discussion.

Table IV(a) shows, as expected, that in the case of pool heating, a simple black-paint one-glass collector is best. It is clear that the addition of a honeycomb (collector 11) is only an added economic burden. It can probably be demonstrated that in some cases (e.g., no wind) it would be more cost effective to have no cover sheet for collectors which are to be used for pool heating.

If collector performance were not the sole selection criterion for a collector that will produce hot water, then a honeycomb collector (collector 11, 12) or a selective two-glass collector (collector 7) would be chosen (table IV(b)). However, on the basis of cost and practicality, it is believed that a black paint two-glass collector (collectors 1, 13 to 15) is the best choice.

Since heating and air conditioning have essentially the same requirements as regards temperature difference ($T_i - T_a$), they are grouped

together in table IV(c). The best performing collector for this type of duty is the black-nickel two-glass collector (collector 7). Close behind collector No. 7 is the flat black-paint-honeycomb two-glass collector (No. 12). An additional factor to be considered for No. 12 collector is the transmission losses at other than normal incidence of solar flux due to the mylar honeycomb. A factor which needs more consideration is the reliability (life) of the black nickel selective coating. The reliability of such a coating needs proving out before collectors utilizing this coating may be considered dependable. The use of selective coatings to cut down radiation losses becomes even more evident at the temperatures needed for solar Rankine system performance. This is clear in the performance ranking shown in table IV(d). The efficiency levels of the better performing collectors for a Rankine system are the same as those of the A/C-heating case.

Collector performance parameters. - Collector performance parameters of five collectors based on the correlations according to equations (2) to (4) are shown in table V. These collector parameters permit a determination of the "why" a collector performed the way it did. Collectors 7 and 13 are basically the same with exception of the coating used on the absorber plate. This basic sameness in construction is reflected in nearly the same values of F' and F_R and in equal values for the glass transmittance (τ). Since the absorptivity for the two collectors is identical, their difference in performance is attributable to the black nickel-coated collector (7) having a lower heat loss coefficient (U_L) than that of the black paint-coated collector (13). Comparing collector No. 7 with collector No. 9, it can be seen that the greatest single factor contributing to the latter's lower performance was the lower value of absorptivity. Table V also demonstrates that the value of absorptivity determined from the intercept of curves such as that of figure 4(a) compares well with the determination of absorptivity from spectral reflectivity measurements.

Incident angle effect. - It was suggested above in the discussion of performance ranking that a final judgment on a honeycomb collector as a high temperature collector would have to await considerations of incident angle effects. Figure 6 shows the correlation curves for the black paint

honeycomb collector (No. 12) at radiation incident angles of zero and 41 degrees. The lower intercept of the curve for 41 degrees is due to window reflection losses and transmission losses due to the mylar honeycomb. The effect of the honeycomb on transmission losses is best judged by running a test on the collector with and without the honeycomb. The results of these tests for incident angles of zero and 41 degrees are shown in table VI. Since the heat loss from a given collector remains unchanged when the collector support stand is rotated about the vertical axis (tilt is constant) for different incident angles, the efficiency change of a given collector is directly related to the values of $\alpha\tau$ listed in table VI. Table VI shows that for an incident angle of 41 degrees use of honeycomb causes a 9-percent decrease in performance as compared to a normal incident condition. Without a honeycomb this relative change in performance is four percent. Because of this transmission loss effect due to the honeycomb, a better basis for performance ranking would be that based on all-day performance.

Future efforts. - Collector testing of different collector types will be continued with the following additions to the test provided:

1. Tests for partial and total diffuse radiation.
2. Standard collector heat capacity test.

A comparison will be made between the simulator tests and collector tests in actual conditions. This comparison will gage the simulator's ability to "simulate" and determine if the performance results obtained with the simulator can be used for predicting collector performance under actual conditions. This would allow calculation for all-day collector performances which would form an excellent basis for the performance ranking of collectors.

SUMMARY OF RESULTS

Fifteen collector types have been given rankings based on their performance in the NASA-LeRC simulation facility. Performance rankings are based on the function a collector is expected to perform. The best

performers in each category of pool heating, hot water, A/C and heating and solar Rankine are as follows:

A. Pool heating
   1. Black paint - one glass

B. Hot water
   1. Black paint plus honeycomb - one or two glass
   2. Black nickel - two glass
   3. Black paint - two glass

C. Absorption A/C or heating
   1. Black nickel - two glass
   2. Black paint plus honeycomb - one or two glass

D. Solar Rankine
   1. Black nickel - two glass
   2. Black paint plus honeycomb - two glass

An evaluation of collector performance by an inspection of collector performance parameters indicated that simply reducing collector heat loss will not guarantee a good performing collector. Some collectors which used selective coatings to reduce radiation losses were found to have lower than expected performance due to a lower than desired value of absorptivity.

For any given application, the final collector selection should be determined from information on collector cost, collector reliability and collector performance based on all-day conditions.

REFERENCES

1. Vernon, R. W.; and Simon, F. F.: Flat-Plate Collector Performance Determined Experimentally with a Solar Simulator. Presented at International Solar Energy Society, Annual Meeting, Fort Collins, Color., Aug. 19-23, 1974.
2. Simon, F. F.; and Harlamert, Paul: Flat-Plate Collector Performance Evaluation. The Case for a Solar Simulation Approach. NASA TM X-71427, 1973.

3. Yass, Kenneth; and Curtis, Henry B.: Low-Cost, Air Mass 2 Solar Simulator. NASA TM X-3059, 1973.

4. Simon, F. F.: A Comparison Under a Simulated Sun of Two Black-Nickel-Coated Flat-Plate Solar Collectors with a Nonselective-Black-Paint-Coated Collector. TM X-

SYMBOLS

C_p	fluid heat capacity, Btu/lb, ^oF
F'	collector plate efficiency factor, dimensionless
F_R	collector plate heat-removal efficiency, dimensionless
G	flow rate of collector fluid, lb/hr-sq ft of absorber surface
q_i	incident direct solar radiation, Btu/hr-ft^2
$\overline{T}_f$	average collector fluid temperature, ^oF
T_i	fluid inlet temperature, ^oF
T_o	fluid outlet temperature, ^oF
$\overline{T}_p$	average collector plate temperature, ^oF
T_a	ambient temperature, ^oF
U_L	overall collector heat loss coefficient, Btu/hr-ft^2, ^oF
α	collector surface absorptivity, dimensionless
η	collector efficiency, dimensionless
τ	effective transmittance
θ_i	solar incident angle, degrees

Superscript:

$\overline{\ }$	average conditions

TABLE I. - COLLECTOR TYPES TESTED

Collector	Absorber panel material
1. LeRC Black paint, two glass	Copper
2. Barber CuO, one glass	Copper
3. Barber CuO + honeycombs, one glass	Copper
4. Beasely CuO, two glass	Copper
5. Honeywell/LeRC No. 1, black nickel, one glass	Aluminum
6. Honeywell/LeRC No. 1, black nickel, two glass	Aluminum
7. Honeywell/LeRC No. 2, black nickel, two glass	Aluminum
8. MSFC black nickel, one Tedlar	Aluminum
9. MSFC black nickel, two Tedlar	Aluminum
10. Honeywell/LeRC No. 3, black paint, one glass	Aluminum
11. Honeywell/LeRC No. 3, black paint + honeycomb, one glass	Aluminum
12. Honeywell/LeRC No. 3, black paint + honeycomb, two glass	Aluminum
13. Honeywell/LeRC No. 3, black paint, two glass	Aluminum
14. Martin Marietta, black paint, two glass	Aluminum
15. Trantor, black paint, two glass	Steel

TABLE II. - NASA-LEWIS SOLAR SIMULATOR SUMMARY

Radiation source,
- 143 Lamps, 300 W each
- GE-type ELH, tungsten-halogen Dichroic coating
- 12^{o} Total divergence angle

Test area,
- 4 by 4 ft, maximum

Test condition limits,
- Flux; 150 to 350 Btu/hr-ft^2
- Flow; up to 1 gal/min (30 lb/hr-ft^2)
- Inlet temp; 75^{o} to 210^{o} F
- Wind; 0 to 10 mph at 75^{o} F

TABLE III. - COMPARISON OF SOLAR SIMULATOR AND AIR-MASS 2 PERFORMANCE

		Air-mass 2 sunlight	Simulator
Energy output, percent	Ultraviolet	2.7	0.3
	Visible	44.4	48.4
	Infrared	52.9	51.3
Energy uses	Absorptivity (Selective surface)	0.90	0.90
	Glass transmission	.85	.86
	Al mirror reflectivity	.86	.88
	Solar cell efficiency, percent	12.6	13.4

TABLE IV. - COLLECTOR PERFORMANCE RANKING

Collector	(a) Pool heating		(b) Hot water		(c) Absorption, A/C or heat		(d) Solar Rankine	
	Coll. No.	η^*	Coll. No.	η^*	Coll. No.	η^*	Coll. No.	η^*
1. LeRC Black paint, 2 glass	10	83%	11	62%	7	45%	7	34%
2 Barber CuO, 1 glass	11	83	7	60	12	43	12	32
3. Barber CuO + honeycombs, 1 glass	2	80	12	58	11	41	11	27
4. Beasely CuO, 2 glass	3	80	1	55	1	35	1	22
5. Honeywell/LeRC No. 1, Bl-Ni, 1 glass	1	75	13, 14	53	13, 14	33	13, 14	18
6. Honeywell/LeRC No. 1, Bl-Ni, 2 glass	12	73	15	52	15	31	6	17
7. Honeywell/LeRC No. 2, Bl-Ni, 2 glass	13, 14	73	10	51	6	28	15	11
8. MSFC Bl-Ni, 1 Tedlar	7	71	2	51	5	25	5	10
9. MSFC Bl-Ni, 2 Tedlar	5, 15	70	3	51	9	24	9	7
10. Honeywell/LeRC No. 3, Bl-Pt, 1 glass	6	61	5	48	4	23	4	5
11. Honeywell/LeRC No. 3, Bl-Pt + honeycomb, 1 glass	4	59	6	45	2, 3	23	8	4
12. Honeywell/LeRC No. 3, Bl-Pt + honeycomb, 2 glass	8	57	4	41	10	21	2, 3	3
13. Honeywell/LeRC No. 3, Bl-Pt, 2 glass	9	54	9	39	8	17	10	0
14. Martin Marietta, Bl-Pt, 2 glass			8	37				
15. Trantor, Bl-Pt, 2 glass								

* q_i = 250 Btu/hr ft^2; T_a = 80^o F. Absorption A/C or heat; q_i = 250 Btu/hr ft^2; T_a = 80^o F, 0^o F.

TABLE V. - COLLECTOR PERFORMANCE PARAMETERS

Collector	F'	F_R	$\overline{U_L}$ (Btu/hr ft^2) ^oF	τ, Per cover	α_{meas} [a]	α_{cal} [b]	$\eta_{A/C}$ [*], percent
LeRC Black paint, 2 glass (1)	----	0.95	0.88	0.87	0.97	----	35
Beasley CuO, 2 glass (4)	----	.90	.85	.86	.86	----	23
Honeywell/LeRC Bl-Ni, 2 glass (7)	0.96	.94	.56	.89	.95	0.92	45
Honeywell/LeRC Black, 2 glass (13)	.97	.93	.80	.89	.95	.93	33
Marshall Bl-Ni, 2 Tedlar (9)	.99	.95	.69	.86	.73	.79	24

[a] Measured with spectrophotometer.

[b] Calculated using experimental value of $\alpha\tau$.

[*] $T_1 = 200^o$ F; $T_A = 80^o$ F; $q_i = 250$ Btu/hr ft^2.

TABLE VI. - EFFECT OF INCIDENT ANGLE

Collector	Incident angle, θ_i	$\alpha\tau$
Black paint Honeycomb, 2 glass (12)	0^o	0.78
	41^o	.71
Black paint 2 glass (13)	0^o	0.78
	41^o	.75

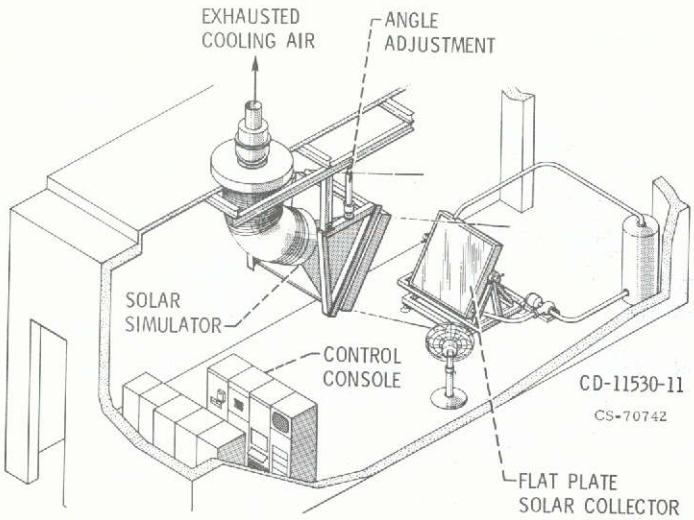

Figure 1. - Indoor test facility.

Figure 2. - Indoor facility used to experimentally determine solar collector performance.

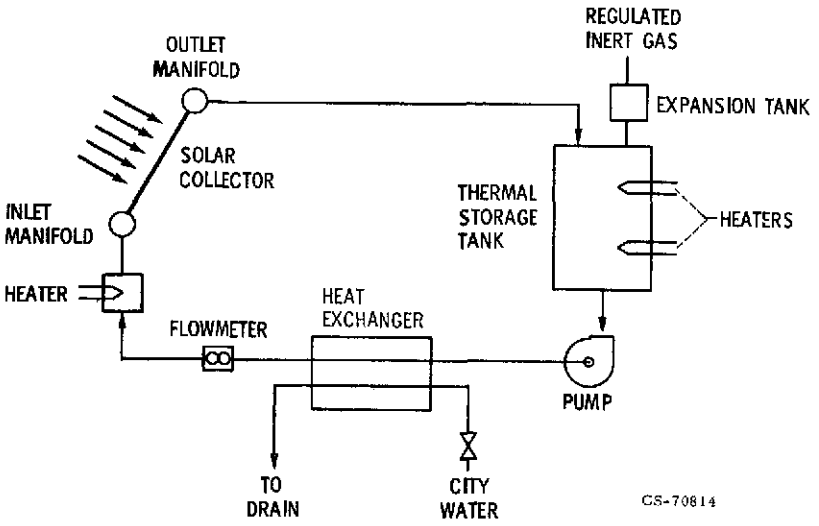

Figure 3. - Schematic of liquid flow loop.

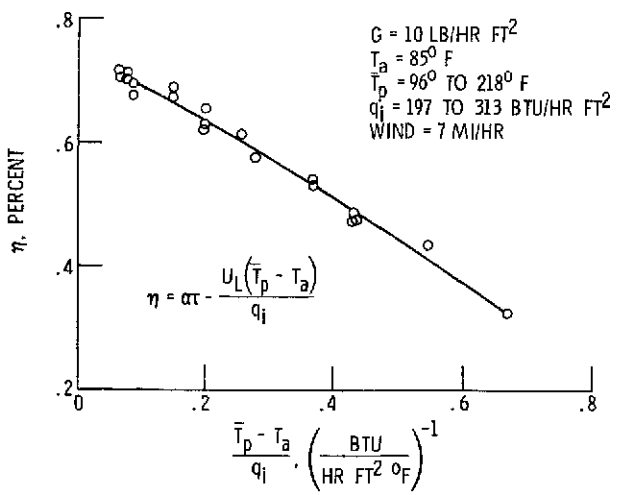

(A) HONEYWELL/LeRC BL Ni 2 GLASS.

Figure 4. - Collector performance correlation.

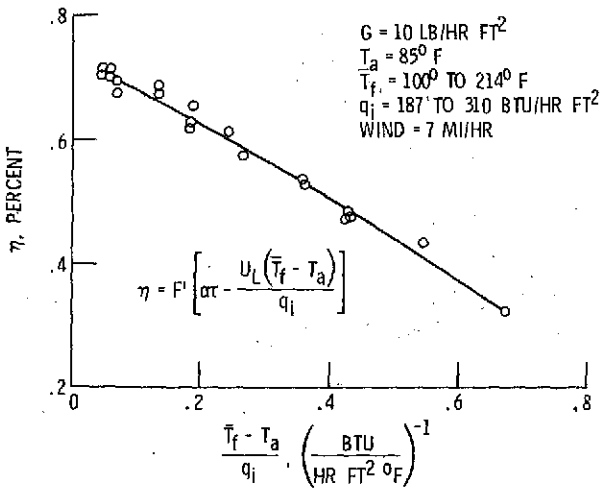

(B) HONEYWELL/LeRC BLACK Ni 2 GLASS.

Figure 4. - Continued.

E-8205

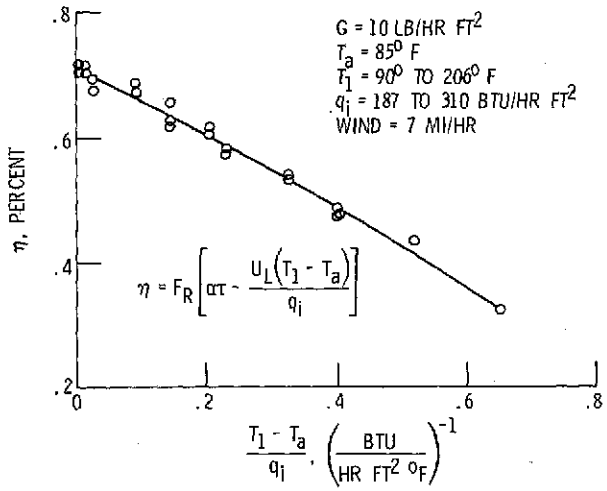

(C) HONEYWELL/LeRC BL Ni 2 GLASS.

Figure 4. - Concluded.

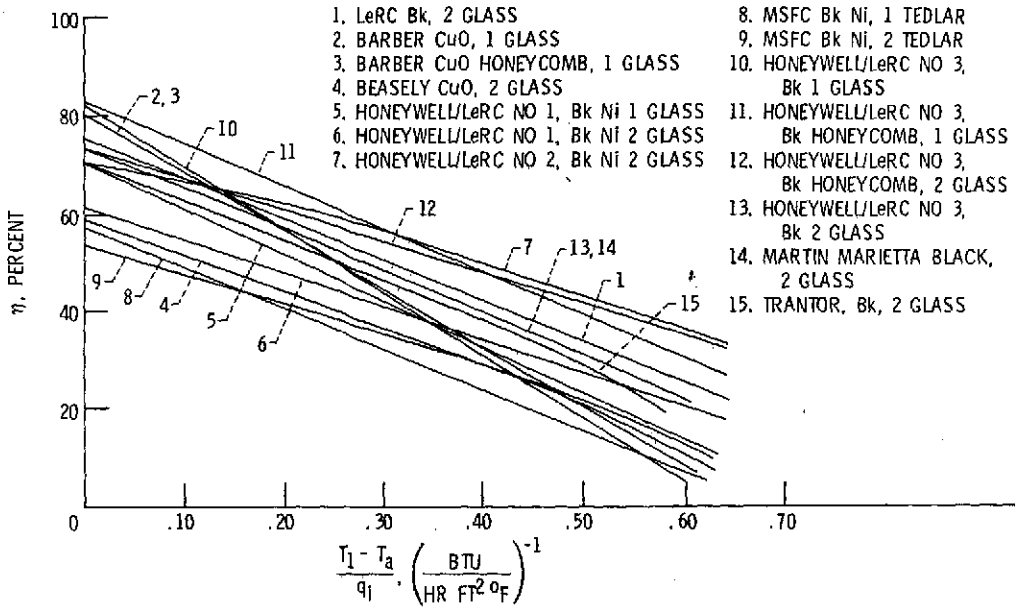

Figure 5. - Results of collector performance tests with NASA-Lewis solar simulator.

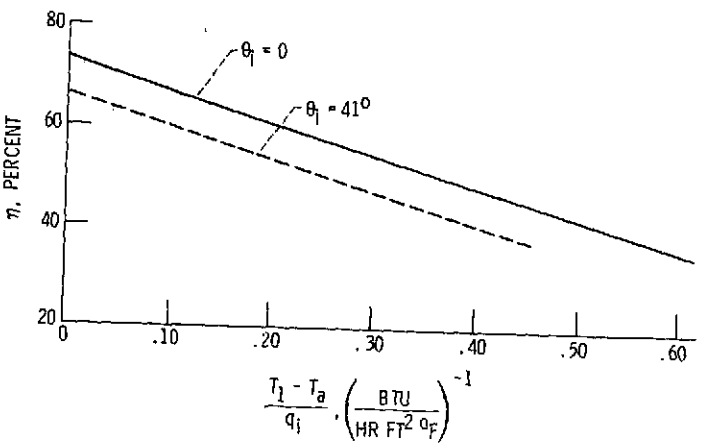

Figure 6. - Effect of incident angle on the performance of a honeycomb collector (no. 12).